Computing unambiguous TEC and ionospheric delays using only carrier phase data from NOAA's CORS network

Dru A. Smith
National Geodetic Survey, NOS/NOAA
Silver Spring, Maryland 20910, USA.

Abstract-A new method for computing absolute (unambiguous) levels of Total Electron Content (TEC) and subsequently the L1 and L2 phase delays of GPS is presented. Unlike previous computational methods, this one relies solely upon dual frequency, ambiguous carrier phase data without any reliance on pseudo-range, a-priori values or other external information. The only requirements for this method are that the ionosphere is assumed to lie in a two-dimensional shell of constant ellipsoidal height, and that the GPS data come from a network of ground stations, geographically separated so as to allow satellites to be viewed by a variety of stations at overlapping times.

The usefulness of this method and its application toward nowcasting and forecasting of the ionosphere are also discussed.

I. INTRODUCTION

It is a well accepted fact that dual-frequency carrier phase data is currently the most accurate data for computing precise positions with the Global Positioning System. However, both integer ambiguities and the Total Electron Content (TEC) along the receiver-satellite path are frequency dependent; and both of these values prevent an absolute and immediate computation of precise position from carrier phase data alone.

Many methods exist for either removing the ionosphere, or mixing in pseudo-range data, or computing both ambiguities and ionosphere delay using lengthy observing sessions. However, in this paper, a method for unambiguously computing the absolute level of TEC, from a network of ground stations and only using ambiguous carrier phase data is being presented. With TEC data computed, the burden of determining integer ambiguities should be significantly reduced [1,2]. In most studies, however, the presumption is that data, including the ionosphere, are processed in double difference mode. This study goes beyond that, actually computing absolute values of TEC from ambiguous carrier phase data.

While the method presented does require the assumption of a two-dimensional "shell model" of the ionosphere, independent checks confirm that the data coming from this method are generally accurate, though with some study still needed to resolve some discrepancies with coarse global ionosphere models. The method presented is fast, and can be kept updated over time using a sequential least squares adjustment as the data change (as new satellites rise and old ones set).

II. ASSUMPTIONS AND DEFINITIONS

This paper makes use of the simple shell model of the ionosphere. In this model, the three-dimensional ionosphere, with TEC measured in electrons/m^3, is compressed to a shell at a fixed ellipsoidal height (often picked as the location approximating the largest real density of electrons). The compression takes place in the direction perpendicular to the shell and leaves the ionosphere with a TEC that is expressed in electrons/m^2 (see Figure 1). For this paper, the shell is fixed at a height of 300 km.
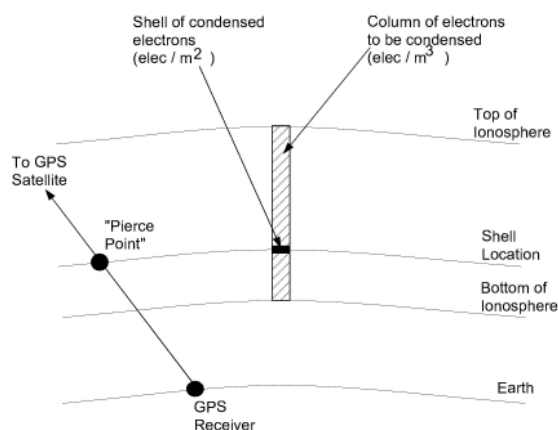

Fig. 1. Sketch of the relationship between 3-D electron density and the compression to a 2-D shell, showing the definition of a pierce point.

With the ionosphere shell model in place, consider next the line connecting a GPS receiver with a GPS satellite, at any given data collection epoch. The intersection of this line with the ionosphere will be called a <u>pierce point</u> (see Figure 1). If one maps the pierce points generated this way, from the rise of satellite above the horizon to its setting below the horizon, a <u>track</u> is generated, such as that seen in Figure 2.
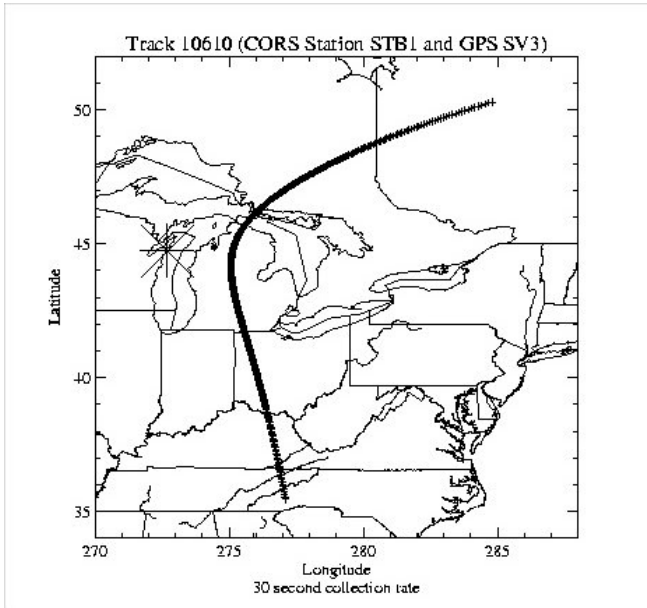
Fig. 2. Track 10610 formed when station SBT1 tracks GPS SV 3 from rise to set. Day 193 (July 12) of 2002. Station SBT1 is shown by the large asterisk.

Consider now a close-up on the ionosphere, at a particular pierce point (see Figure 3).
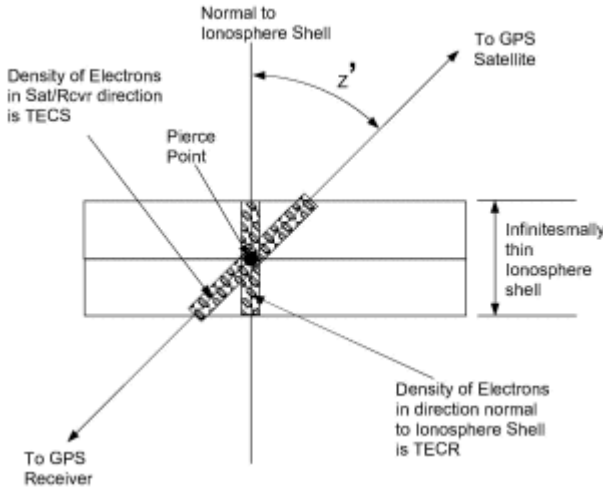

Fig. 3. Close-up of the ionosphere shell at a pierce point, showing the difference between the two electron densities TECS and TECR

An important distinction will be made between the density of electrons seen along the receiver-satellite direction (TECS) and the density of electrons seen in a direction radial to the ionosphere shell (TECR). They are related by the piercing angle, z' as:

$$TECS = TECR / \cos z' \qquad (1)$$

It has long been understood that the phase advance (or negative delay) experienced by GPS receivers is a function of the number of electrons through which the L1 and L2 carrier waves pass. That is, the number of cycles of advance, due to the ionosphere, can be written as a function of TECS and frequency as:

$$I_1 = -\frac{\kappa}{f_1 c} TECS = (0.853)TECS \qquad (2)$$

$$I_2 = -\frac{\kappa}{f_2 c} TECS = (1.095)TECS \qquad (3)$$

where:

I_1, I_2 = cycles of phase delay in L1 and L2 respectively
c = speed of light [299,792,458 m / s]
f_1, f_2 = frequency of L1 and L2 respectively [1,557,420,000 and 1,227,600,000 cyc / s]
TECS   = density of electrons in receiver-satellite direction in TECU (10^{16} elec / m^2)
κ = 40.3 x 10^{16} (m cyc^2 / TECU / s^2)

While the ionospheric delay experienced at a receiver is a function of TECS, it would be most helpful to somehow generate a map of TECR, so that any vector connecting a GPS satellite to a GPS receiver, piercing the ionosphere, can have its TECS value (and thus its ionospheric delay) computed by simply knowing TECR and computing the piercing angle z' from the satellite orbit.

As a final definition, consider the case when two tracks come "near" one another. In the field of altimetry, if they actually crossed geographically this would be called a "crossover". In this study, however, the term crossover will not be applied to strict crossing, but rather to any two pierce points, on separate tracks, that fall within some acceptably small tolerance (in *both* space *and* time) of one another.

III. THE MATHEMATICAL MODEL

At any epoch "i", the relationship between the geometric range (^{i}d) and the measured range (^{i}r) from a GPS receiver to satellite can be expressed (for L1 and L2 respectively) as:

$$^{i}r_1 = {}^{i}d + c^{i}\Delta t + {}^{i}I_1 / \lambda_1 + {}^{i}T + {}^{i}m_1 \qquad (4)$$

$$^{i}r_2 = {}^{i}d + c^{i}\Delta t + {}^{i}I_2 / \lambda_2 + {}^{i}T + {}^{i}m_2 \qquad (5)$$

where

r_1, r_2 = Measured range to satellite on L1 and L2 respectively
d = Geometric range to satellite
$c\Delta t$ = Range error due to clock errors
λ_1, λ_2 = Wavelengths of L1 and L2 respectively
T = Range error due to troposphere
m_1, m_2 = Range error due to carrier phase multipath error on L2 and L2 respectively

Now, presume that a GPS receiver is tracking carrier phase data on L1 and L2. At acquisition of L1 and L2, it will compare its internal oscillator with the number of L1 and L2 cycles received and report a more or less nonsensical (i.e. "ambiguous") number of cycles. Presuming it does not lose lock, it will continue to generate an internal L1 and L2 cycle count, and compare the changes in cycles of its internal count to those cycles received from the GPS satellite. The difference between received and internal cycles can be interpreted as the change in measured range (r) due to satellite motion. Equivalently it could be considered the change in geometric range (d) plus the change to all error sources. Thus between two epochs i and j:

$$^{i,j}\Delta\varphi_1\lambda_1 = {}^{i,j}\Delta r_1 =$$
$$^{i,j}\Delta d + c\,{}^{i,j}\Delta\Delta t + {}^{i,j}\Delta I_1 / \lambda_1 + {}^{i,j}\Delta T + {}^{i,j}\Delta m_1 \tag{6}$$

$$^{i,j}\Delta\varphi_2\lambda_2 = {}^{i,j}\Delta r_2 =$$
$$^{i,j}\Delta d + c\,{}^{i,j}\Delta\Delta t + {}^{i,j}\Delta I_2 / \lambda_2 + {}^{i,j}\Delta T + {}^{i,j}\Delta m_2 \tag{7}$$

where $^{i,j}\Delta\phi_1$ and $^{i,j}\Delta\phi_2$ are the differences, in cycles, between the number of L1 or L2 cycles generated inside the receiver with the number of cycles received from the GPS satellite, over the time period from epoch i to epoch j. (This is basically the difference between any two observed values of L1 or L2 between two epochs). Now, if one subtracts equation 7 from equation 6 then only frequency dependent terms will remain:

$$^{i,j}\Delta\varphi_1\lambda_1 - {}^{i,j}\Delta\varphi_2\lambda_2 =$$
$$({}^{i,j}\Delta I_1 / \lambda_1 - {}^{i,j}\Delta I_2 / \lambda_2) + {}^{i,j}\Delta\Delta m_{1,2} \tag{8}$$

Going forward, the assumption will be made that m_1 and m_2 are small, and also that the difference between m_1 and m_2 is small enough to be neglected [3,4]. Then, applying equations 1, 2 and 3 to equation 8 and solving for the TECS term we end up with the following:

$$^{i,j}\Delta TECS = {}^{j}TECS - {}^{i}TECS =$$
$$\left(\frac{1}{\kappa}\right)\left(\frac{1}{f_1^2} - \frac{1}{f_2^2}\right)^{-1}\left({}^{i,j}\Delta\varphi_1 - {}^{i,j}\Delta\varphi_2\right) \tag{9}$$

This equation shows that if we take the difference (in time) of the difference (in frequency) of L1 and L2 cycle changes (between internal and received) we have an unambiguous measure of the difference (in time) of the electron density as seen along the receiver-satellite path (TECS). What this means is that if we plot a curve of TECS versus time for a particular track, we know the *shape* of TECS for that track, but we are *missing a single bias* which would define the absolute values of TECS for that

track. This is exemplified in Figure 4 where five (of an infinite number) of TECS curves have been drawn for one particular track (designated number 10,610 of some 12,585 tracks during the day). Note that all 5 curves have the same shape, but with an unknown absolute value.
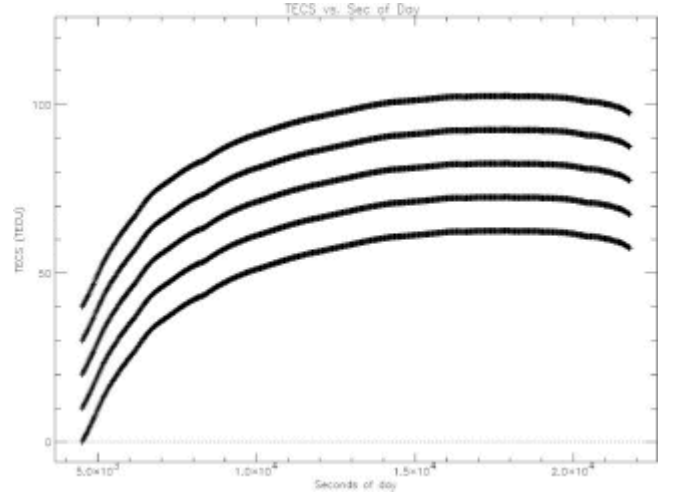

Fig. 4. Five possible versions of TECS for track 10610 showing identical shape, but variable absolute values.

Remember that the goal of this paper is to model TECR values, not TECS. An equation for ΔTECR as a function of ΔTECS can be written as:

$$^{i,j}\Delta TECR = {}^{j}TECR - {}^{i}TECR =$$
$$^{j}TECS \cos{}^{j}z' - {}^{i}TECS \cos{}^{i}z' =$$
$$^{i,j}\Delta TECS \cos{}^{j}z' + {}^{i}TECS(\cos{}^{j}z' - \cos{}^{i}z') \tag{10}$$

The disconcerting conclusion of equation 10 is that we may not simply determine the unambiguous temporal changes of TECR along a track the way we did for TECS (the dependence of $^{i,j}\Delta TECR$ upon $^{i}TECS$ causes the ambiguity). This ambiguity, arising from the cos z' mapping between TECS and TECR prevents us from determining even the shape of TECR curves, let alone their absolute values. This is shown in Figure 5 where the five TECR curves corresponding to the five TECS curves of Figure 4 are plotted. Notice that they are not parallel curves (like TECS was), but rather have shapes that depend upon their absolute values.

While this at first may seem a point of difficulty, as it turns out the non-uniqueness of the shape of TECR curves is exactly the key information needed to determine unambiguous TECR data from a network of GPS stations. The basic idea is explained below.
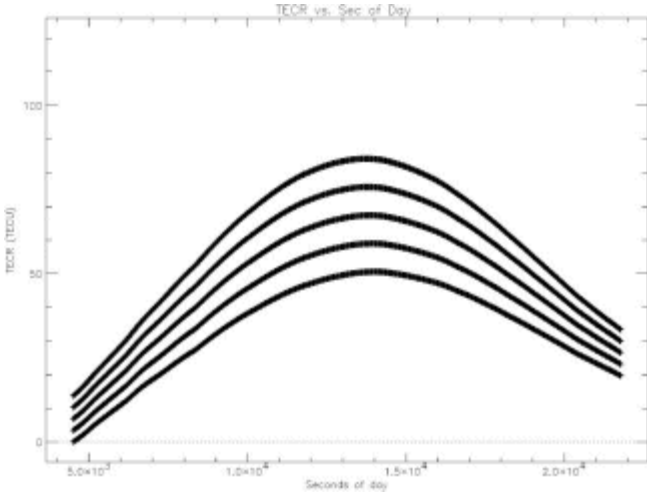
Fig. 5. Five possible versions of TECR for track 10610 (corresponding to the TECS curves of figure 4) showing differing shapes dependent upon absolute values.

Consider the case of 3 GPS tracks (call them 1,2 and 3), generated by 3 GPS/receiver combinations, and distributed in such a way that the 3 tracks have 3 crossovers (call them A, B and C), effectively forming a "triangle" on the ionosphere shell (see Figure 6).
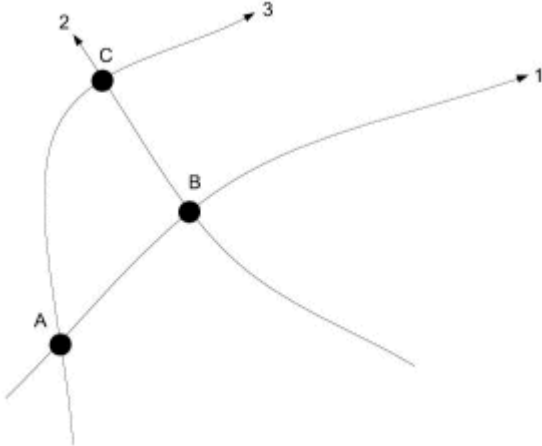

Fig. 6. A "triangle" formed by 3 tracks and 3 crossovers.

As previously stated, we know the shape of the TECS curve along each of the three tracks, but do not know the absolute value. Put another way, each of the 3 tracks (1, 2 and 3) has 1 unknown bias (b_1, b_2 and b_3). In fact, let's define b_i as the actual value of TECS on track i at the very first point on that track. If we knew that bias, we could compute the absolute values of TECS (because we know ΔTECS along the track) and knowing the absolute levels of TECS we can compute the absolute levels of TECR. So in this example, 3 tracks mean 3 unknowns. But how do we solve for them? As it turns out, each crossover acts as a unique constraint for the system. The three crossovers at A, B and C provide the following constraints on the system:

$$ {}_1^A TECR = {}_3^A TECR (= {}^A TECR) \qquad (11) $$

$$ {}_1^B TECR = {}_2^B TECR (= {}^B TECR) \qquad (12) $$

$$ {}_2^C TECR = {}_3^C TECR (= {}^C TECR) \qquad (13) $$

That is, the TECR values at a crossover must be unique, independent of track. Notice that while all of our actual track information is in the form of ΔTECS values, the actual constraints on the system are on TECR. So, in the notation used above, let's write out the conversion from TECR to TECS and see how the unknown biases fit into the picture:

$$ {}_1^A TECR = {}_1^A TECS \cos {}_1^A z' = $$
$$ (b_1 + {}_1^A \Delta TECS) \cos {}_1^A z' \qquad (14) $$

$$ {}_3^A TECR = {}_3^A TECS \cos {}_3^A z' = $$
$$ (b_3 + {}_3^A \Delta TECS) \cos {}_3^A z' \qquad (15) $$

$$ {}_1^B TECR = {}_1^B TECS \cos {}_1^B z' = $$
$$ (b_1 + {}_1^B \Delta TECS) \cos {}_1^B z' \qquad (16) $$

$$ {}_2^B TECR = {}_2^B TECS \cos {}_2^B z' = $$
$$ (b_2 + {}_2^B \Delta TECS) \cos {}_2^B z' \qquad (17) $$

$$ {}_2^C TECR = {}_2^C TECS \cos {}_2^C z' = $$
$$ (b_2 + {}_2^C \Delta TECS) \cos {}_2^C z' \qquad (18) $$

$$ {}_3^C TECR = {}_3^C TECS \cos {}_3^C z' = $$
$$ (b_3 + {}_3^C \Delta TECS) \cos {}_3^C z' \qquad (19) $$

Substituting equations 14-19 into equations 11-13, and converting to matrix (Y=A X) form yields:

$$ \begin{bmatrix} {}_1^A\Delta TECS\cos{}_1^A z' - {}_3^A\Delta TECS\cos{}_3^A z' \\ {}_1^B\Delta TECS\cos{}_1^B z' - {}_2^B\Delta TECS\cos{}_2^B z' \\ {}_2^C\Delta TECS\cos{}_2^C z' - {}_3^C\Delta TECS\cos{}_3^C z' \end{bmatrix} = \begin{bmatrix} -\cos{}_1^A z' & 0 & +\cos{}_3^A z' \\ -\cos{}_1^B z' & +\cos{}_2^B z' & 0 \\ 0 & -\cos{}_2^C z' & +\cos{}_3^C z' \end{bmatrix} \begin{bmatrix} b_1 \\ b_2 \\ b_3 \end{bmatrix} \qquad (20) $$

This system of linear equations has a similarity to those used, for example, in solving altimetric crossovers or geodetic leveling problems. In the case of altimetry and geodetic leveling however, the A matrix contains only +1, -1 and 0 and is thus non-invertible without additional constraints. In contrast, the cosines in our A matrix allow for an inversion. In simplest terms, this means that even though we only know ΔTECS (that is, the shape or temporal changes of TECS) on a track and we only know that TECR must be identical at the crossovers (independent of track), we can compute one unique absolute value of TECS at the beginning of each track (b_1, b_2 and b_3). Knowing this value, we are then able to compute all TECS values for the entire track and subsequently all absolute TECR values for the entire track.

Therefore, within the confines of our opening assumptions, an unambiguous solution for TECR, based

solely on ambiguous carrier phase data, has been found. It is entirely due to the (cos z') mapping between TECS and TECR that this is possible. As it turns out, this mathematical relationship holds for any number of tracks that form a closed polygon, not just for triangles, since the number of sides (tracks) of a polygon must equal the number of vertices (crossovers), and thus would provide a unique and solvable system.

However, while the above triangular example offers a unique solution, it offers no redundancy. But if the situation is made just slightly more complex, say by adding a 4th track, crossing tracks 1 and 2 at points D and E respectively (forming another triangle, with common vertex B) we begin to build up redundancy. See Figure 7.
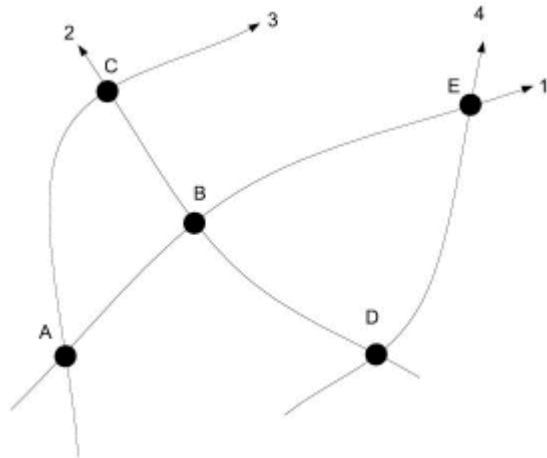

Fig. 7. Adjoining "triangles" showing 4 tracks (unknowns) and 5 crossovers (observations) and thus redundancy

In this case, we now have 4 tracks (with unknowns b_1, b_2, b_3 and b_4) but 5 crossovers (observation equations), and thus a Least-Squares Adjustment (LSA) can be performed on this redundant system. This buildup of redundancy grows as the number of tracks grows, since each new track can be expected to cross more and more existing tracks, adding multiple crossovers (observations) to the system while only adding 1 unknown bias for the new track.

Given the fact that a complex network of tracks should yield more crossovers than tracks, it seems that the ideal application of this model is toward a large network of dual frequency carrier phase GPS receivers, which are continuously operating and spaced geographically so that their tracks cross, but offer some wide spatial distribution in the ionosphere.

IV. THE CORS NETWORK

The National Geodetic Survey (NGS), part of the National Oceanic and Atmospheric Administration (NOAA), coordinates a network of continuously operating reference stations (CORS) that provide GPS carrier phase and code range measurements in support of 3-dimensional positioning activities throughout the United States and its territories (see Figure 8).
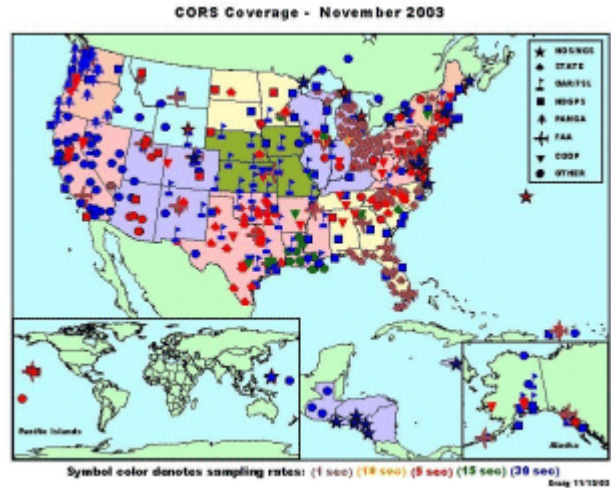

Fig. 8. The CORS Network

The CORS system benefits from a multi-purpose cooperative endeavor involving many government, academic, commercial and private organizations. New sites are evaluated for inclusion according to established criteria. The data are collected at various rates (1, 5, 10 or 30 seconds) and then transmitted (with varying latencies) to NGS for coordinate computation, data distribution and archival. However, these data are also perfect for modeling the ionosphere using the mathematical model outlined in the previous section.

A.   *Data collection and cleaning*

For the results presented in this paper, data from day 193 (July 12) of 2002 were used, when CORS had 307 stations collecting data.

The data were collected from the CORS archive, in RINEX (Receiver Independent Exchange) format. Then the raw carrier phases were transformed into ΔTECS data, cleaned and sorted into tracks.

Each CORS station has one RINEX file for the 24 hour period of day 193, year 2002. The data for each individual satellite were collected together first, then points missing either L1 or L2 were thrown out. A ten degree vertical angle cut off was used to maximize both crossovers and spatial distribution and also so the impact of points low to the horizon might eventually be studied. Tracks with fewer than 10 successive data epochs were considered too short to be useful and were dropped.

For the remaining tracks, the ΔTECS values were computed using equation 9. These data then were investigated for cycle slips by discarding any ΔTECS values which were considered physically or statistically unrealistic. For this study, "physically unrealistic" was set at 0.2 TECUs / km (Paul Spencer, NOAA, personal communication). Gradients exceeding this value were fixed, if possible, using weighted averages of neighboring gradients on the same track.

Finally, any loss of data for longer than 5 minutes constituted the end of one track. The "cleaned" gradients, for the single CORS/Satellite combination were then given unique track numbers, and the next CORS/Satellite combination was similarly processed. All in all, the number of "cleaned" tracks for this one day was 12,585, averaging about 1008 points (data epochs) per track.

V. INITIAL TESTS

To test the rigor of the mathematical model of section III, small tracknets (groups of tracks connected via crossovers) were formed and their biases solved in a LSA. Then the modeled TECR values were converted to double-difference (DD) values and compared to independently computed double-differenced (DD) TECR values found through DD solutions at the Geosciences Research Division of NGS (G. Mader, NOAA, personal communication). A variety of LSA methods were tested. Presuming some closed polygon could be found in the tracknet, then no a-priori information was needed in the LSA, and the carrier-phase data could entirely control the absolute level of TECR in the adjustment. However, it was seen as useful to determine the impact of some a-priori information, since this would be needed in any LSA of a tracknet where no closed polygon of tracks could be formed, or even in a case where a-priori information might be desired, though not necessary. This second case presumes that the a-priori information is reliable and will add useful information to the LSA.

A-priori information on the TECS biases for each track can be obtained most quickly through a fitting of carrier phase TECS data to pseudo-range TECS data. However, this presumes that the pseudo-range data is available (not always true) and that the multi-path errors average to zero (generally not true) so that the mean offset of phase and pseudo-range would be an unbiased estimate of the true bias in the phase-based TECR values. Considering the number of possible biases in pseudo-range data, it is not totally surprising that the results using only the carrier phase data generally ended up better than those that introduced a-priori information from phase/pseudo-range fitting.

Figures 9 and 10 show two different examples of phase/pseudo-range fitting. In Figure 9, one can clearly see that the phase data fits very accurately through the highly noisy pseudo-range data; though, considering how noisy the pseudo-range data are, it's difficult to know what non-zero biases are hidden in that data set. In Figure 10, we can see that the fit is even less clean and further calls into question the usefulness of a phase/pseudo-range a-priori estimate.
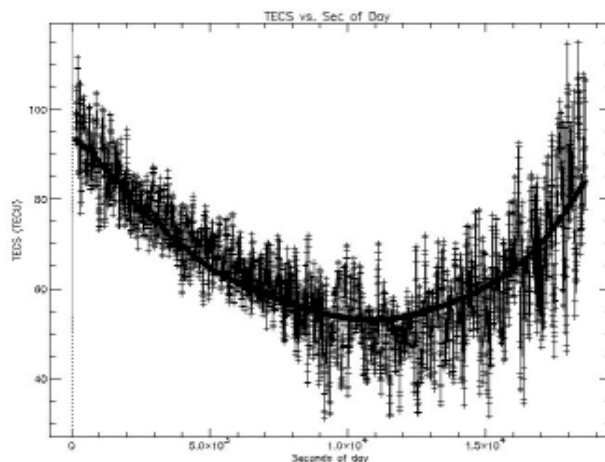

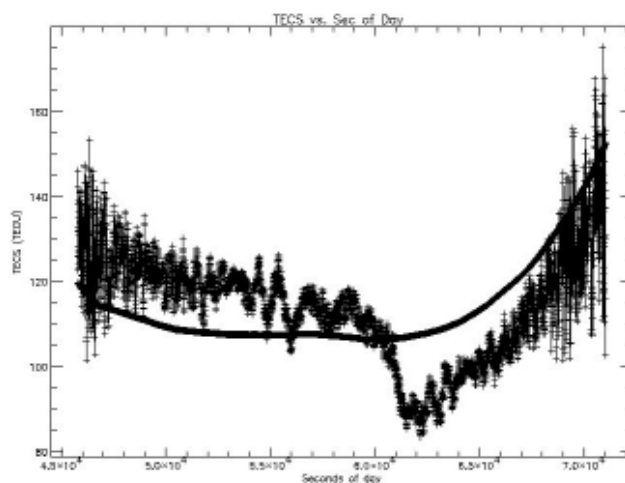Fig. 9. A good fit between phase and pseudo-range based TECS values on track 174.

Fig. 10. A poor fit between phase and pseudo-range based TECS values on track 8366.

Many small (10-100 tracks) tracknets were formed and tested before moving on to a larger adjustment. These tests served mostly to prove the methodology, rather than provide significant insight into the ionosphere itself. All results were similar, therefore only one example will be presented here.

A pair of stations, viewing a pair of satellites were chosen to form a double difference. In this example, they are CORS stations GODE and RED1, receiving data from GPS SV1 and SV2. The four tracks (designated 4300, 4303, 9484 and 9487) formed by combining the 2 stations and the 2 satellites will be called the "DD tracks". It is the intention of this small adjustment to investigate the best way to arrive at TECS values on the 4 DD tracks. First off, it was necessary to find a small "net" of tracks where they are all interconnected and which contains the 4 DD tracks. Options in the adjustment are whether or not to have a 'closed polygon' in the net, and whether to use none, some or all of the a-priori bias estimates on the tracks in the net. Table 1 shows the track numbers used in the tracknet.

Track #	CORS name	GPS SV #	Hours of day	Track used in solution?				A-priori info used?			
				1	2	3	4	1	2	3	4
4300	GODE	1	0.00 - 5.18	x	x	x	x	x	x		
4303	GODE	2	0.00 - 5.93	x	x	x	x	x	x		
9484	RED1	1	0.04 - 5.15	x	x	x	x	x	x		x
9487	RED1	2	0.04 - 6.05	x	x	x	x	x	x		
2253	CONO	22	0.00 - 4.62	x	x	x	x				
10146	SHK1	1	0.04 - 5.08	x	x	x	x	x	x		
11416	UIUC	25	0.00 - 2.70	x	x	x	x				
12565	YOU1	20	0.04 - 2.42	x	x	x	x	x	x		
2224	COLB	25	0.00 - 2.91		x	x	x				
11580	UPO1	22	0.00 - 4.85		x	x	x		x		

Track #	Solution 1	Solution 2	Solution 3	Solution 4
4300	± 3.5	± 2.9	± 0.1	± 1.2
4303	± 8.8	± 4.7	± 0.2	± 2.1
9484	± 9.3	± 4.6	± 0.2	± 2.0
9487	± 9.4	± 3.1	± 0.1	± 1.3
2253	± 13.6	± 5.9	± 0.3	± 2.5
10146	± 9.7	± 3.3	± 0.1	± 1.4
11416	± 6.5	± 4.9	± 0.2	± 2.0
12565	± 6.1	± 3.9	± 0.2	± 1.6
2224	-	± 4.3	± 0.2	± 1.7
11580	-	± 3.0	± 0.1	± 1.2

Four different solutions were investigated based on various options mentioned above, but always with the goal being TECR values on the four DD tracks. Note that the double difference exists from GPS time 0.04h to 5.15h, allowing over 5 hours of continuous data for testing. The first 8 tracks were chosen because they are the smallest set of tracks that all connect one to another, such that the tracknet contains all 4 DD tracks. However, these 8 tracks do not form a closed polygon on the ionosphere shell; they contain only 7 crossovers and therefore would require a-priori information to solve. The additional 2 tracks (2224, 11580) were chosen because they combine with the first 8 tracks to form the smallest tracknet that contains all 4 DD tracks and contains a closed polygon. In fact, these 10 tracks contain 2 closed polygons[1]. The 10 track tracknet contains 11 crossovers, and therefore could be solved without any a-priori information.

Solution 1 contained the first 8 tracks (thus no polygons) and a-priori estimates on all tracks that had pseudo-range data (6 of 8). Solution 2 contained all 10 tracks (thus 2 polygons) and a-priori estimates on all tracks that had pseudo-range data (7 of 10). Solution 3 contained all 10 tracks and no a-priori estimates. Solution 4 contained all 10 tracks and only one a-priori estimate (track 9484). These small tracknets were adjusted and biases solved for. The formal (a-posteriori) error estimates of the biases for each track, converted into cycles of delay on L1 are presented in Table 2.

One may draw some immediate conclusions from Table 2. The improvement from solution 1 to solution 2 indicates that simply having a closed polygon in the tracknet has stabilized the solution significantly. Additionally, the improvement from solution 2 to solution 3 shows that the a-priori information (based on pseudo-range/phase fitting) is actually degrading the adjustment, causing dispersion in the adjusted tracknet. Leaving the a-priori data out entirely in solution 3 seems to strengthen the tracknet and yield a very rigid set of adjusted biases. Finally, the slight degradation from solution 3 to solution 4 is due solely to adding just 1 piece of a-priori information. This further exemplifies the degrading nature of unnecessarily adding pseudo-range data.

After these adjustments were performed, TECR values were converted to cycles of delay on L1 for the entire track, and double differenced. These were then provided to GRD for comparison to delay estimates that came from an independent double-difference adjustment for the coordinates of GODE and RED1 (Mader, ibid). The results are shown in Figure 11.

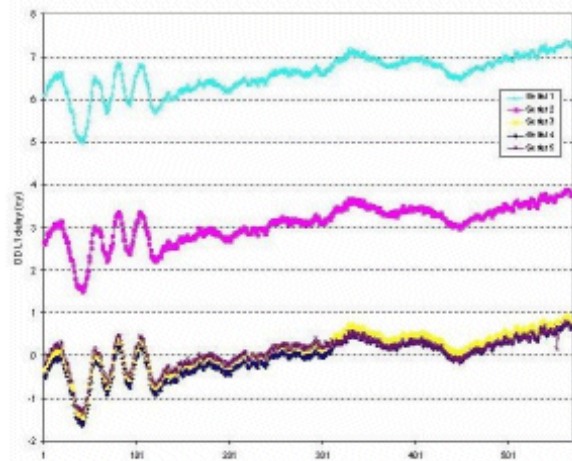Fig. 11. Comparison between 4 different solutions for the DD TECR values and a 5th independent solution from NGS positioning software showing agreement between solutions 3 and 4 (yellow and dark blue) with the independently computed DD TECR values (dark red).

---

[1] The two polygons are 8 sided and 3 sided, respectively, and have the following tracks as sides: 9484-2253-10146-11580-2224-4300-11416-12565 and 9487-10146-11580.

As seen in Figure 11, solutions 3 and 4 have the best agreement to the independent DD solutions, which further strengthens the argument that no a-priori information needs to be put into the modeling of the ionosphere. The agreement between solution 3 and the 5th (independent) DD L1 delay values is at the 0.01 cycles value (RMS) and is remarkable, considering TECR values were first computed as absolute values, and then converted to DD values and absolutely no a-priori information was used in solution 3. Numerous other examples, not detailed here, were performed with similar conclusions.

VI. FULL DAY ADJUSTMENT

With the confidence that the small tracknet adjustment tests provided, the next step was to attempt to compute a 24 hour adjustment of all biases for all tracks that had at least one connection to a single, master tracknet. Logical search operations were coded to find such a tracknet. As it turns out, of the 12,585 tracks that were formed by CORS on day 193 of 2002, there were 8298 which formed a master tracknet (that is any of those 8298 tracks could be traced, via crossovers, to any other of the 8298 tracks). The criteria for a crossover was that some point on one track lay within a small space-time window [0.1° x 0.1° x 60 seconds] as a point on another track. Of those tracks that did not connect to the master tracknet, most were either very short, very low on the horizon, provided by a distant CORS station (e.g. Hawaii, Alaska, Caribbean) or some combination of these factors.

Of the 8298 tracks (unknowns) that formed that master tracknet, there were 16,896 crossovers (constraints), thus providing a very redundant system of linear equations. Sparse matrices were the obvious choice for this adjustment. Each row of the A matrix corresponded to one constraint (cross-over). The only non-zero elements in any given row of the A matrix are in the 2 columns which correspond to the 2 tracks which make the crossover. Although no immediate pattern of non-zero elements arises from this situation, we nonetheless have only 0.024% of elements of A that are non-zero.

Using the sparse matrix routines of NGS' "HEART OF GOLD" software [5], this system of equations was solved for all 8298 track biases in 30 seconds, and the sparse profile elements of the dispersion matrix of the adjusted biases following in a further 10 minutes of computations.

Once the adjusted biases and their dispersions were computed, we checked the post-adjusted crossovers to see how well the master tracknet closed. Table 3 shows the statistics of the post-fit crossovers. Table 4 shows how well the formal error estimates of the adjusted biases came out.

TABLE 3
POST-FIT CROSSOVER STATISTICS FOR MASTER TRACKNET (TECUS)

#	Ave	STD	RMS	Min	Max
16,896	-0.004	±0.51	0.51	-3.7	+4.0

TABLE 4
STATISTICS OF A-POSTERIORI STANDARD DEVIATIONS FOR POST-FIT MASTER TRACKNET BIASES (TECUS)

#	Ave STD	Min STD	Max STD
8298	±1.1	±0.22	±10.7

In addition to these statistics, it is useful to consider the actual TECR values for every point on every track in the master tracknet. Applying the adjusted TECS bias of each track to the known ΔTECS values, and then generating TECR values, the following statistics are found in Table 5.

TABLE 5
POST-FIT TECR VALUES FOR ENTIRE 24 HOUR MASTER TRACKNET (TECUS)

#	Ave	STD	RMS	Min	Max
10,613,013	14.90	±6.03	16.07	-7.5	+58.4

As seen in Table 5, the adjusted TECR values are reasonable (on average) but with poor outliers (below zero or above 50 TECUs). The negative TECR values, however, are rare, (0.08% of all TECR values) as are those above 50. Aside from these outliers, we can show the generally believable nature of the ionosphere more clearly. The adjusted TECR values were averaged in 2 hour intervals and plotted over 24 hours. Additionally, values for TECR over the same geographic area from 5 IGS (International GPS Service) computational centers (COD, EMR, ESA, JPL and UPC) were downloaded from their archive and plotted. See Figure 12.
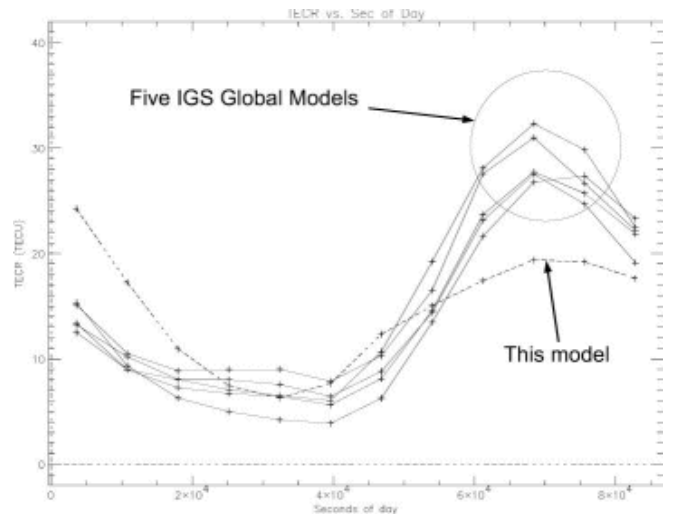

Fig. 12. The 5 IGS models compared to the method of this paper showing good agreement at night and early morning

Note that the agreement is much better between this method and the global models at night and morning (central parts of plot). The disagreements for the late afternoon (left side of plot) and late morning (right side of plot) could be due to a number of sources. First, this method used over 300 stations just in the USA, while all 5 global models averaged only 120 stations for the entire globe. Additionally, the geographic and temporal spacing for the global models was 5° x 2.5° x 2 hours, whereas this method

models the ionosphere at every data epoch (1, 5, 15 or 30 seconds) on the densely packed tracks themselves. Additionally, the global models assume an ionosphere shell height of 450 km while this study used 300 km. Because the cut-off angle used in this paper was 10 degrees, the errors in mapping TECS to TECR via equation 1 can lead to errors in remote tracks, such as those over the ocean areas where only a few (shoreline) stations can see the rising satellites through the ionosphere, and then only low on the horizon. Finally, the disagreement occurs during the most active time of the ionosphere itself as well, which also propagate into the errors of using equation 1.

Considering the good agreement between this method and the 5 global methods during at least the night/morning half of the day, and the explainable (and possibly repairable) sources of disagreement during the rest of the day, Figure 12 is encouraging as a first step. This is especially so when one considers that no pseudo-range fitting or other a-priori methods of solving for the biases were used. At the very least, the method is well-suited to double difference ionosphere modeling, and shows great promise as a method for absolute ionosphere modeling, provided further study can be performed on the disagreements of Figure 12.

At this point, the ionosphere has been modeled, but at discrete times (data epochs) and discrete locations (tracks). We then turned our attention to the question of how best to use such data, and subsequently, how best to distribute it. Clearly, visualization of the ionosphere would be an aid to anyone interested in understanding or using this model. That would generally imply transforming our values onto a grid. However, one of the ultimate goals of this project was to provide, at the best possible accuracy, values of ionospheric delay to surveyors using a GPS receiver in the field. Going from tracks to a grid back to a surveyor's track would mean two sources of interpolation error. Going directly from the adjusted master tracknet to a surveyor's track would seem to be a more accurate path.

Ultimately, both were investigated, and their advantages and disadvantages are discussed in the next sections.

VII. GRIDDING

Putting aside for the moment the singular application of providing ionosphere delays to individual surveyors, it would seem that the obvious path to provide our ionosphere model to the general public would be in the form of a grid of TECR values at discrete points in time. Such a grid lends itself to easy distribution, interpolation, analysis, conversion to other units, comparison to other ionosphere models and of course, visualization. The problem of transforming random points to a grid has a long history. Splines, collocation and polynomials all have advantages and disadvantages. What was seen as important here was finding a method that would allow the spatial and temporal connections to remain in the grids, while allowing fast and accurate gridding. The method chosen for this paper was

one of many possible methods and is certainly not meant to be the final choice. However, for the sake of expediency, a few quick experiments lead to the following scheme:

Step 1: Fit a 3-D polynomial of degree and order 1 (called TECR0) to the TECR data:

$$TECR0(\phi, \lambda, t) = \sum_{i=0}^{1} \sum_{j=0}^{1} \sum_{k=0}^{1} a_{i,j,k} \phi^i \lambda^j t^k \qquad (21)$$

Step 2: Remove TECR0 from TECR
Step 3: Block-mean the residual data in blocks of size 0.1° x 0.1° x 15 min
Step 4: Transform block-means to 2-D gridded values every 15 minutes using splines in tension [6], and a tension parameter of $T = 0.1$
Step 5: Restore TECR0 to gridded residuals

and, for the sake of visualization only, to avoid serious edge effects:

Step 6: Mask the final grids by using a 100km buffer around all ϕ / λ locations which had at least one pierce point over the 24 hour period.

One could chose many different versions of this scheme (different polynomial, or using an a-priori grids (such as the IGS global grids); a different tension parameter; a different size for block-means) or a different scheme altogether (e.g. Fourier series; Collocation). The emphasis of this study is not to study which of these schemes is best – that will come in a future paper. The emphasis is to show that even the simplest scheme can yield results that are both visually pleasing and statistically reasonable.

Figure 13 shows the final, gridded and masked ionosphere values for year 2002, day 193, at time 13500 sec. This is one of 97 grids which make up the entire 24 hour period.
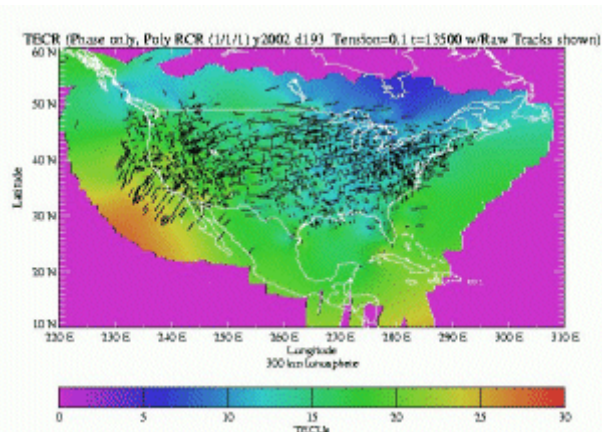

Fig. 13. Modeled TECR data (masked to remove edge effects) at t=13500 sec, with raw tracks shown for the 15 minute period surrounding this time.

All 97 grids were animated, and made available at http://www.ngs.noaa.gov/IONO/f.gif. Such animation

serves two purposes. It is an invaluable tool for analysis of actual ionospheric activity, but also allows a very quick method of determining outliers. We are currently in the process of re-cleaning the data based on this animation and the information it yielded. It should be noted that the resolution, in both space and time, of this ionosphere grid is much better than anything previously seen in global models.

Once the grids were computed, the question arose of how well we could go from a grid back to a track. (This would obviously be the way our grids would be used). Again, we adopted the strategy of testing the simplest solution first, knowing that more elaborate schemes of interpolation should only improve upon the initial results. Therefore, taking the grids, and using a basic tri-linear interpolation of the closest 8 points, we attempted to re-create the original adjusted master tracknet. The statistics of that experiment are shown in Table 6.

TABLE 6

MISFIT OF ORIGINAL TRACKNET TO TRACKNET RE-GENERATED FROM GRIDDED DATA (TECUs)

#	Ave	STD	Min	Max
10,613,013	+0.001	±0.38	-7.8	+8.8

As can be seen in Table 6, the ability to go from tracknet to grid and back to tracknet can be done, in a very simple method to almost perfect accuracy and with a precision of 0.38 TECUs. Certainly such a precision could be improved with better gridding and interpolation algorithms, but on the other hand, even the best of these methods may not improve the ability to correctly predict the ionosphere in locations removed in space and time from the data of the master tracknet. Such areas arise when GPS receivers are outside of (but near) the USA, or even in the USA itself in areas where CORS is sparse (such as the north central region; see Figure 8).

Given that the gridded data appears to be a useful for visualization and even a reasonable method of accessing the information contained on the tracks themselves, we turn our attention next to the possibility of accurately predicting ionosphere data on a track by directly interpolating off of the master tracknet itself.

VIII. INTERPOLATION VIA A TIN

It was already seen that, in addition to being a good visual tool, a gridded ionosphere model can be a reasonable predictor, at least to a precision of 0.38 TECUs. It was hoped that by skipping the gridding altogether, an even greater precision could be achieved. The scheme relies on a method quite like that of a Triangulated Irregular Network (TIN).

Consider 3 CORS stations that form a triangle; inside this triangle is a 4th GPS receiver. If, at the same epoch all four of these receivers are receiving data from the same GPS satellite, and if the 3 CORS stations can compute the ionosphere through the adjustment of the master tracknet, it stands to reason that we should be able to estimate what the

ionosphere seen by the 4th GPS receiver should be, based on the 3 surrounding stations.

To test this hypothesis, each CORS station contributing to the master tracknet was investigated as follows: First, a variety of "surrounding triangles" (if any) were found, based on all other CORS stations in the master tracknet. Four types of triangles were studied to see if the choice of triangle would have a noticeable advantage over the other types. The four types of surrounding triangles are outlined in Table 7.

TABLE 7

DIFFERENT TRIANGLE TYPES FOR TIN EXPERIMENTS

Triangle Type	Description
1	with the smallest area
2	with the smallest maximum side
3	with the smallest maximum distance from CORS to central receiver
4	with the largest minimum angle

When the triangles were defined, the adjusted master tracknet was run through the comparison program. Basically it would make sure that all 4 CORS receivers were seeing the same satellite at the same epoch. It would then use the TECR values from the 3 corner CORS stations to approximate the TECR value at the central CORS station, using the geometry of the triangle on the ground. (An alternate, and possibly more robust, solution would be to re-compute the triangular geometry formed by the 4 pierce points at every epoch, but this has the disadvantage of needing the relations between all 4 stations re-computed every epoch). This interpolated TECR value was then compared with the actual value of TECR from the central CORS site as seen in the master tracknet. The results are shown in Table 8.

TABLE 8

STATISTICS OF TRACK-REGENERATION VIA TIN METHODS, BASED ON 4 TRIANGLE TYPES (TECUs)

Triangle Type	# points	Ave	STD	Min	Max
1	1,950,266	-0.010	±0.28	-10.8	+11.8
2	2,761,325	-0.005	±0.25	-11.1	+11.6
3	2,569,277	-0.006	±0.25	-11.1	+12.0
4	1,933,781	-0.029	±0.29	-10.2	+11.6

A few important things can be gleaned from Table 8. First, not every CORS station in the master tracknet could be surrounded by 3 other such CORS stations. As such, those data were not part of this analysis. Additionally, since CORS stations can have data rates of 1, 5, 15 or 30 seconds, it is possible for significant data to be skipped in this analysis if one of the CORS stations has a lower data rate than the other 3, since common epochs were a requirement for comparison.

Finally, it should be noted that independent of the type of triangle chosen, this method yields results that are around 0.25 TECUs, which is an improvement over the gridding method of section VIII.

One must be careful not to presume that the ability of either the gridding or TIN methods to re-create the original TECR data is a measure of absolute accuracy. Certainly both the gridding and TIN methods have high precision, but the accuracy of the method itself will only come through independent verification of this model. Currently, the best comparisons available are from coarse (in both space and time) global models, but the difficulties with such a comparison have already been outlined.

In the future, actual application of this method toward directly reducing the time needed to resolve integer ambiguities will be the best test and guidance for future directions.

IX. CONCLUSIONS AND FUTURE DIRECTIONS

This paper was an introduction to a new method for unambiguously computing the total electron content of the ionosphere using ambiguous carrier phase GPS data only. While certain assumptions were required for this method to work, notably the use of the constant-height shell model, it nonetheless was a mathematically sound method. There were no tricks, iterations or other ways to get around the ambiguity of carrier phase data. Biases were found during daylight hours between this model and global models at the 5+ TECU level. But these appear to be solvable with future research. Aside from these biases from the global model, the method in this paper appears to have a precision approaching 0.25 TECUs. By converting TECUs into cycles of delay on L1 and L2, we can say that the method described in this paper has the ability to accurately model the ionosphere to a precision of 0.21 cycles on L1 (~ 4.0 cm) and 0.27 cycles on L2 (~ 6.6 cm). When double-differenced, a precision of 0.01 TECU was found.

The adjustment of thousands of crossovers for the solution of thousands of biases in only 30 seconds meant that this method can be easily adapted to a sequential least-squares method, where old tracks can be updated and new tracks allowed to enter the master tracknet and sequential adjustments performed in sequential epochs. All that was required for a track to yield valid ionosphere data was that a single crossover must exist between a track and the master tracknet. Once the single bias for the track is known, all TECR values along that track are therefore determined in absolute value. Whether this ionosphere model is used in a grid or a TIN method, its speed of computation, precision, and dependence on an existing GPS network make it a powerful new tool for ionospheric information distribution. But serious questions remain, all of which are slated to be covered in future studies. Questions to be answered include: How many CORS stations are needed before no further ionospheric information is gained? What is the best method to test and validate the data? How does this model behave on days of significant ionospheric activity? How can we resolve the existing discrepancies with the global models? And, of greatest interest to geodesists, what improvement is gained in integer ambiguity resolution?

These questions are all valid, but the primary question of this study has been answered: It is mathematically possible, almost trivial, to compute the unambiguous value of TEC in the ionosphere from ambiguous carrier phase GPS data only. The next phase is testing this method for applicability to the integer ambiguity resolution problem, and discovering why biases exist between this method and the global models.

REFERENCES

[1] Odjik, D., 2000: Weighting ionospheric corrections to improve fast GPS positioning over medium distances, Proceedings of the Institute of Navigation 2000 meeting

[2] Teunissen, P.J.G. and D. Odjik, 2003: Rank-defect integer estimation and phase-only modernized GPS ambiguity resolution, Journal of Geodesy, v. 76, pp. 523-535.

[3] Wanninger, L. and M. Manja, 2001: Carrier-phase multipath calibration of GPS reference stations, NAVIGATION, v. 48, n. 2, pp. 113-124.

[4] Langley, R.B., 1996: Propogation of the GPS Signals, Lecture Notes in Earth Sciences, v. 60 (Kleusberg and Teunissen Eds.)

[5] Milbert, D.G.,1984: HEART OF GOLD: Computer routines for large, sparse, lease squares computations. NOAA Technical Memorandum NOS NGS-39, 1984.

[6] Smith, W. and P. Wessel, 1990: Gridding with continuous curvature splines in tension, Geophysics, v. 55, n. 3, pp. 293-305.